

RADIATION-PHYSICS ASPECTS OF NAL CONSTRUCTION

Prepared for the AEC Advisory Panel on Accelerator
Radiation Safety

M. Awschalom, T. Borak, P. J. Gollon, and D. Theriot

May 26, 1970

1. Introduction

This report summarizes the radiation-physics work carried out at the National Accelerator Laboratory as part of the construction of the 500-BeV synchrotron. The report covers shielding design and estimates of residual radioactivity of the accelerator and external-beam components and structures up to the targets. Design of the experimental areas is now in progress and is not reported here. General procedures and assignment of responsibilities in radiation safety and monitoring are discussed; this part of the report is necessarily incomplete, because only a small part of the total accelerator system is now producing beam and detailed procedures for much of the accelerator have not been completely fixed. For a complete description we refer the reader to the NAL Design Report,¹ with the warning that some of the plans outlined there have been outmoded by subsequent work.

The NAL synchrotron is of the third generation of multi-BeV proton accelerators and, therefore, considerable experience in accelerator construction and operation has been brought to bear on its design.



There are also new developments in accelerator technology, such as the long straight section and the electrostatic extraction septum, that have been incorporated in the design. With this experience and new developments, we expect a decrease in undesired beam losses and a better understanding of their origin.

An important result that comes from experience at other accelerators is that there is a direct relationship between the shield thickness needed while the accelerator is operating and the residual radioactivity after shutdown. That is, a greater beam loss at a point in the accelerator requires a greater shield thickness to contain the resulting radiation, but it also means that there will be greater residual radioactivity near the beam-loss point. This residual activity will make maintenance of the accelerator much more difficult. Our general approach to beam loss in accelerator design has therefore been to decrease the beam loss rather than to increase the shielding so that we will always be able to maintain it conveniently. It is our firm intention that if there is undesired beam loss at some point, we will operate the accelerator at lower intensity until the causes of the beam loss are understood and cured. We have therefore designed the shielding for these expected beam losses.

At the same time, we have attempted to provide a safety factor. There is provision and space for local shielding within the accelerator housings around beam-loss points. There is also provision in the

design of the housings for additional exterior shielding, should that be necessary.

2. General Description

The National Accelerator Laboratory site encompasses 6,826 acres in DuPage and Kane Counties, approximately 30 miles west of downtown Chicago. The site is roughly a rectangle, approximately 3 miles long on each side. It is very flat land, varying in elevation less than 50 feet over the entire site.

Figure 1 is a schematic plan of the Laboratory. The main-accelerator ring, approximately a circle 1.24 miles in diameter (3.9 miles circumference) is located in the southwest quarter of the site. At the point of closest approach, the ring is approximately 2,000 feet from the southern boundary of the site.

The main accelerator is divided into six superperiods, each with a long straight section having a clear drift space of 167 feet between magnets. One long straight section is utilized for injection and extraction and one for the rf accelerating system.

Injection into the main accelerator from the booster, an 8-BeV rapid-cycling synchrotron, and extraction of the accelerated beam take place in straight-section A at the northwest part of the ring. This straight section is housed in a reinforced-concrete structure called the Transfer Hall. The extracted beam goes northeast from the Transfer Hall to a splitting station, where all or part of it can be sent to any of

three target stations. The 200-MeV linear accelerator that feeds the booster, the main accelerator, the external proton-beam enclosure, and the targets are all shielded. We shall discuss this shielding in detail in this report.

The clustering of functions in the injection-extraction area is purposeful. The scale of the accelerator is so large that we feel a strong attempt must be made to foster communications between different parts of the effort. To this end, the Central Laboratory, where a significant part of the total Laboratory staff will work, is located in this area, between the low-energy end of the linac and the extraction end of the Transfer Hall. The Central Laboratory will be a 16-story structure of approximately 400,000 gross square feet, containing offices and light laboratories and shops. The location of many administrative and service functions in this area places stringent limitations on stray radiation generated during injection and extraction.

3. Injection, Extraction, and Targeting

3.1 200-MeV Booster Injection. The 200-MeV beam from the linac is transported down from 740 ft elevation to the 726.5 ft elevation of the booster. Two 200-MeV beam dumps are provided for linac studies and for trimming the linac beam for efficient injection into the booster. They are discussed in Sec. 4.3 below.

Four turns are injected into the booster, using a programmed orbit bump to move protons away from the injection septum. Some

schemes used with this system could result in a loss of up to 20% of the injected particles. This loss would be localized on a shielded beam-scrapers system. The beam will be debunched from the 200-MHz linac frequency during transport and injection. It will be rebunched at the initial booster frequency of 33 MHz. This bunching and rf capture will be done "adiabatically" during the slow field rise at the bottom of the sinusoidal field excitation. This slow capture will reduce beam loss to an estimated 5% or less (not including the up to 20% loss mentioned above).

Provision is also made for cutting out and dumping approximately two of the 84 booster bunches at 200 MeV, in order to leave a gap for use in synchronization with the main ring. These bunches will be transported to a beam dump in the booster.

3.2 8-BeV Injection. Protons accelerated to full energy in the booster will be synchronized in radio frequency and phase with the main-accelerator rf system, which is on during injection. The beam will be extracted from the booster in a single turn with no loss by a fast-kicker magnet system. They will be injected into the main accelerator by a kicker-magnet system of very similar design. Since they will be injected into existing rf buckets, there should be no beam loss in this transfer process. An 8-GeV beam dump is provided for booster-accelerator studies. There will also be an abort system for proton energies of approximately 500 MeV.

3.3 Main-Accelerator Abort System. An abort system will be provided to dispose of the proton beam at any time during acceleration, should its parameters be outside acceptable limits. This system will utilize kicker magnets to steer the beam into a locally shielded dump in a medium straight section. The abort system itself has not yet been designed in detail, but it is not expected to present any technical difficulties.

3.4 Full-Energy Extraction. Both fast (single-turn) and slow-extracted beams will be provided in the same beam line to the targets. The fast-extracted beam will utilize a system of kicker magnets to move the beam into the extraction channel. The slow beam will utilize a third-integral resonant extraction system, with sextupoles placed around the main ring.

The heart of the system is the septum device. The purpose of the septum is, of course, to separate the fields in the extraction channel from those in the accelerator itself, in order that protons can continue to circulate in the accelerator until they are moved outward beyond the septum and go down the extraction channel. Septum devices in high-energy accelerators have in the past been magnetic. The septum in a magnetic device is usually a current-carrying sheet whose thickness is determined by the necessity for cooling. The minimum thickness achieved has been approximately 1 mm (0.04 in.). Because of manufacturing tolerances, the effective septum thickness is usually somewhat larger.

The septum thickness is important because the fraction of particles lost by striking the septum is directly proportional to it. In the last year, discrepancies between this theoretical statement and experimental results have been resolved. Both Brookhaven and CERN now have agreement between theory and experiment in their slow-extraction systems.

The electrostatic septum can be made considerably thinner than a magnetic device, because it carries no current. Model septum devices have been built at NAL with thicknesses of 0.05 mm (0.002 in.) and successfully operated at fields of 75 kV/cm, twice the nominal design value. The success of the electrostatic-septum concept can be judged by the fact that both Brookhaven and CERN have adopted it for use in their 30-BeV synchrotrons.

A further interesting development is that the septum can be shadowed by a passive system ahead of it, which acts to Coulomb-scatter particles away from the septum and to reduce nuclear interactions. Recent experiments at Brookhaven² have shown that this method improves extraction efficiency.

The beam-extraction systems were designed for 200 and 400 BeV. That is, space is provided so that the 200-BeV system can be extended to 400 BeV by doubling the number of extraction elements. Work is in progress on extraction systems for 500 BeV.

3.5 Beam Splitting and Target Systems. The extracted beam is split

between targets by a system very similar to the beam-extraction system. It is then transported upward from the accelerator level of 725.5 ft to the target level of approximately 745 ft.

Production of radiation in targets is the whole point of the accelerator, so we must be prepared to deal with high radiation levels at these points. The shielding of these areas is discussed in detail in Sec. 4 below. It should also be noted that a system for maintenance and changing of highly radioactive target components has been designed and is in the process of prototype testing.

In this system, components are put into position in a target box by means of a remotely controlled railroad system. Experiments have shown that components can repeatably be located by this system within errors of a few thousandths of an inch. The railroad system will carry radioactive components to a target laboratory, where remote-handling facilities will be available for maintenance, repair, and installation on the railroad car.

4. Shielding Design

In this section, we shall summarize the beam-loss estimates, theoretical considerations, and calculations of the shielding design of the accelerators. As noted in the introduction, considerations of remanent radioactivity are folded in with other requirements of shield thickness. In the following, the linac will be treated separately from the booster and main accelerator. Because of the construction

schedule, the linac calculations were carried out at a different time.

In addition, because of the difference in energies, different calculational methods were used.

Finally, the muon-shielding problem is discussed separately. It is of major interest in backstops, rather than in the accelerators themselves, because of the strong forward peaking of muon production.

4.1 Linac Shielding*

a. Beam-Loss Criteria. The following fractional losses are estimated to occur along the linac:

Between tanks 1 and 2 ($E_p = 10 \text{ MeV}$)	2%--it will occur on graphite scrapers, so will produce no neutrons
Between tanks 2 and 3 ($E_p = 37 \text{ MeV}$)	0.5%--local shielding will be provided
Between other tanks	0.01% per junction, total of 0.06%.

With the local shielding, one might take a total estimated loss of 0.1% as a basis for the design of the fixed shielding. We choose 1% as a safe basis.

The design and maximum expected proton currents are summarized in the table on the following page.

*This section is a summary of Ref. 3.

	<u>Design Values</u>	<u>Maximum Expected Values</u>
Peak Current (mA)	50-75	100
Pulse Width (μ sec)	30	100
Repetition Rate (Hz)	14-15/3.2 or 4.0 sec	15
Current (A)	$5.25-10.5 \times 10^{-6}$	1.5×10^{-4}
Proton Current (sec^{-1})	$3.3-6.6 \times 10^{13}$	9.4×10^{14}

Thus, with the assumed 1% loss, we take as a basis for calculations the following estimates of the loss per unit length $dI/d\ell$:

Design:	$2.4-4.8 \times 10^7$ p/cm-sec
Maximum:	6.8×10^8 p/cm-sec.

The larger figure is used throughout the calculations, giving an additional safety factor in the expected mode of operation.

b. Methods of Calculation. The calculations have been carried out in collaboration with K. O'Brien of the AEC Health and Safety Laboratory. The dose rate outside a thick shield is taken by O'Brien as

$$I = k \left(\frac{dI}{d\ell} \right) / 2\pi R,$$

where k is a constant chosen for each proton energy, shielding material, and depth in the shield, $dI/d\ell$ is the loss above, and R is the transverse distance from the beam line to the observation point. O'Brien has given⁴ tables of the constant k , which we have parameterized for computation.

The linac wall between the equipment gallery and the linac tunnel itself is made of ordinary concrete with a density of 2.3 g/cm^3 . For the berm over the linac tunnel, the soil was compacted to a density of 1.9 g/cm^3 , with a water content of 15%.

c. Shielding. The calculated dose rate one foot inside the Linac Gallery, one foot from the side of the berm, and one foot above the top of the berm are shown in Figs. 2, 3, and 4. Figure 5 shows the calculated required wall thicknesses along the linac. The actual wall thickness used is superimposed. Extra thickness has been added near the 200-MeV spectrometer to permit beam-diagnostic work with total beam losses for short times.

The dose rate outside the berm is calculated to be 0.15 mrem/hr at the high-energy end of the linac at maximum intensity.

d. Shield Penetrations. There are four personnel entrances:

(i) Temporary entrance at about the 20-MeV point. This will be sealed after installation of the second tank.

(ii) 92-MeV entrance. An air-cushion concrete door is located here. The door is as thick as the fixed wall (in units of g/cm^2).

(iii) 200-MeV entrance. The labyrinth at this entrance has a calculated attenuation factor of approximately 4×10^{-7} .

(iv) Low-energy entrance. There could be back-scattering of neutrons giving a dose rate of approximately 0.5 rem/hr at the pre-accelerating column, which is not an occupational area. This dose rate corresponds to the maximum beam-loss rate (6.8×10^8 p/cm-sec), which includes a safety factor of an order of magnitude. If this back-streaming should prove troublesome, a wall of concrete blocks will be built at approximately the middle of the first tank.

There are also twenty-seven 30-inch penetrations of the gallery-tunnel wall for power, utility, and control connections. These penetrations will be partly filled with cables and pipes. Should the neutron flux through them be objectionable, the voids in the penetrations will be filled and they will be locally shielded.

e. Remanent Exposure Rates. Estimates of the remanent exposure rates have been made by Alsmiller et al.⁵ and by Gollon,⁶ by different methods. Their results are presented in the table below.

Exposure Rates in mR/hr at 30 cm from Linac Tanks.

Cooling Times Proton Energy	Gollon		Alsmiller			
	8 hr		8 hr		1 hr	
	I ₁	I ₂	I ₁	I ₂	I ₁	I ₂
38	1.3	0.1				
50	1.5	0.1	2.4	0.2	4.4	0.3
100	6.7	0.4				
150	24	1.7				
200	46	3.3	51	3.7	68	4.8

It can be seen that these rates, although they will require monitoring, do not present problems for normal maintenance, which will occupy only a small fraction of the work week.

4.2 Main-Accelerator and Booster Shielding*

a. Beam-Loss Criteria. It is assumed that 0.1% of the total beam power is lost uniformly at the same point in every synchrotron magnet. The total beam power is 480 kW at 200 BeV and 19.2 kW at 8 BeV. Some losses will occur that are ten times larger than the uniform loss rate and shielding must be provided for these greater losses. In addition, there will be local shielding around particular hot points, such as beam scrapers, extraction septa, and so forth.

b. Remanent Exposure Rate from Beam Loss. The CERN data of Goebel⁸ and BNL data can be summarized for a point loss by the rule-of-thumb formula

$$D_p = 57 P,$$

where D_p is the dose rate in R/hr at a time one hour after shutdown at a distance of one foot, and P is the power loss in kW. By analogy to the electric fields from point and line charges, one may write the dose rate from a line loss as

$$D_L = 114 P,$$

where P is measured in kW per foot and D_L in R/hr at one foot one hour after shutdown. Thus a line loss of 1/114 kW/ft will produce a remanent field of one R/hr at one foot.

At 200 BeV, 1/114 kW/ft corresponds to a proton loss of

* This section is a summary of Ref. 7.

9×10^6 /cm-sec. Alsmiller has calculated⁹ the remanent exposure rate for a line loss of protons on the axis of an iron cylinder. For a loss of 9×10^6 /cm-sec, his result is a dose rate of 0.54R/hr, in excellent agreement with the scaling calculation using the "rule of thumb."

We may therefore use Alsmiller's work to estimate the remanent exposure rate at one foot from the magnets one hour after turnoff. The results are tabulated below.

Remanent Exposure Rate from Average Beam Loss.			
	Booster	Main Accelerator	
Magnet Length	2.8×10^4	4.7×10^5	cm
Proton Loss	5.4×10^5	3.2×10^4	p/cm-sec
Magnet Leg Thickness	50	198	g/cm ²
Exposure Rate	1.9	2.5	mR/hr

This calculation is an overestimate in the sense that it takes all the losses to be at maximum energy. On the other hand, the booster calculation does not include possible beam loss during multi-turn injection, which, depending on the system used, could be as high as 20%. One may scale from the work of Armstrong¹⁰ to find a dose rate of 4.6 to 9.2 mR/hr from this injection loss. Hence, the expected dose rate from the booster is 6.5-11 mR/hr.

Even with the 10-to-1 variation from the average loss, the remanent exposure rates are estimated to be tolerable without additional local shielding.

It may also be noted in this connection that the remanent exposure

rate from the concrete enclosure walls is unimportant because of the low-sodium aggregate used in construction.

The estimated beam losses therefore give rise to tolerable remanent exposures. The same beam losses are used in design of the biological shield.

c. Methods of Calculation. The dose rate dDE/dt in rem/hr outside a thick shield is taken as

$$\frac{dDE}{dt} = \frac{kPS(\ell)}{R^2} \exp\left(-\sum_i \frac{x_i}{L_i}\right),$$

where k is a constant, discussed below, P is the beam loss in kW, x_i is the thickness of the i^{th} shielding material, L_i is the mean free path of the i^{th} shielding material, R is the perpendicular distance from the beam line to the observation point (ft), and $S(\ell)$ is a superposition factor giving multiple-point losses at distances ℓ in terms of single-point losses.

There are several sources in the literature for values of k . We have chosen to use

$$k = 18 \times 10^4 \text{ rem ft}^2/\text{kW-hr.}$$

We choose this value because it is the mean value of the Rutherford and ANL values using point targets in the external beam.

To calculate the superposition factor $S(\ell)$, we have used BNL¹¹ and CERN¹² data. The dose distribution inside the shield is taken in the form

$$Y(Z) = 6.59 \times 10^{-3} \left[\frac{1}{\exp(-Z/A) + C \exp(+Z/B)} \right],$$

where Z, the distance along the beam line, is measured in feet. The constants have the values A = 5.563 ft, B = 22.11 ft, C = 10⁻³. The superposition function SF(Z) is the sum of contributions Y(Z) from multiple points. S(ℓ) is the maximum of SF(Z) (ℓ is the mean distance between corresponding loss points in the magnets). We have summed over 13 Y(Z) functions to find

$$\begin{aligned} S(\ell) &= 4.20 \text{ (Booster)} \\ &= 2.04 \text{ (Main Accelerator)}. \end{aligned}$$

d. Shielding Results. We list below the values used for L_i, the mean free path. We give for comparison the smaller values derived from Bellettini's¹³ measurements with some reasonable assumptions.

<u>Material</u>	<u>Density (g/cm³)</u>	<u>L_i (g/cm²)</u>	
		<u>NAL</u>	<u>Bellettini</u>
Steel		165	120
Heavy Concrete		132	107
Soil (15% H ₂ O)		120	96

We also list the parameters of the accelerators used in the calculations.

	<u>Booster</u>	<u>Main Accelerator</u>	
Nominal Power	19.2	480	kW
General Losses	1.92 × 10 ⁻²	0.48	kW
Number of Magnets	96	954	
Concrete + Soil Shield	926	996	g/cm ²
Steel	100	120	g/cm ²
Distance to pt 1 ft above berm	19	23	ft

We include the variation of 10 times the mean value. Then we find

$$\begin{aligned} \frac{d(DE)}{dt} &= 1 \text{ mrem/hr (Booster)} \\ &= 0.4 \text{ mrem/hr (Main Accelerator)}. \end{aligned}$$

These values are calculated using large values of the mean free path and therefore contain an effective safety factor of close to an order of magnitude.

Thus we calculate a dose rate well below the legal limits for radiation workers for a 40-hr week. We achieve this dose rate with a berm that uses only the material excavated for construction of the tunnels. We may note that the closest portion of the Central Laboratory Building will be approximately 100 feet from the top of the berm. We will therefore have an additional attenuation by a factor 5, even from a line source. This will bring the dose rate at the outside of the Central Laboratory to a level of 0.2 mrem/hr, a level adequate for the general public, even without consideration of the safety factors in the calculations.

e. Accesses.* All booster and main-accelerator accesses were designed for an attenuation of 5×10^{-7} , consistent with the attenuation of the earth shielding. The attenuations were calculated using a Monte Carlo neutron-transport program, ZEUS ALB. 5¹⁵ which generates monoenergetic neutrons randomly and transports them through a

*This section is a summary of Ref. 14.

labyrinth of nearly arbitrary shape. Reflection of neutrons from the concrete walls is treated by the albedo method.¹⁶

As an example, we shall discuss the main-ring major vehicle entrance, shown in Fig. 6. It is a semicircular tunnel in plan view, with an 8 by 8 ft square cross section. The radius of curvature of the inner wall is 50 ft. Only particles produced in a backward direction from the proton beam can travel any significant distance down the curved labyrinth. At the far end of the labyrinth, there is a hoist shaft, stairway, and elevator.

A beam loss was assumed to occur at a point in the accelerator as shown in Fig. 6. The computed neutron flux as a function of distance down the centerline of the tunnel, measured from the point of beam loss, are plotted in Fig. 7. After a short region in which the loss point can be seen directly, the attenuation per unit length is roughly constant. The effect of the short straight tunnel just before the shaft and the sharp decrease in flux around the 90° bend of the shaft can also be seen. The overall attenuation of the labyrinth is 10^{-8} .

The attenuation of the main-ring minor-vehicle accesses with 12-ft inner radius was computed as 2×10^{-7} . Subsequently, the inner radius of the semicircular part of this labyrinth was increased from 12 to 25 feet for architectural purposes. This increase in radius of curvature was more than compensated by the increased length of the semicircle, from 47 to 88 feet.

The attenuation of personnel entrances to the 24 service buildings around the main ring were calculated with and without cul-de-sacs. The overall attenuation of the labyrinth without cul-de-sacs is 2×10^{-7} . These labyrinths are in fact being built with one cul-de-sac, which houses a sump. Their attenuation is calculated to be 7×10^{-8} .

The main-ring personnel-access labyrinth results were used in the calculations of the attenuation of the booster and linac labyrinths. The difference in cross-sectional areas of the labyrinths was taken into account by scaling the centerline distance L of the tunnels to an effective length L_{eff} according to the formula.

$$L_{\text{eff}} = \sqrt{\frac{\text{Area (MR)}}{\text{Area (Boost)}}}.$$

Using this recipe, the overall attenuation of the booster personnel-access labyrinths is 9.2×10^{-8} .

The overall attenuation of the booster major vehicle access is estimated to be 6×10^{-10} . This figure is probably overly optimistic, because the large attenuation of the curved sections is diluted by their relatively short length. Nevertheless, even if this effect makes the estimate too optimistic by two orders of magnitude, there is still an ample safety factor compared with the design attenuation of 5×10^{-7} .

4.3 Work on Beam Dumps

a. Linac Beam Dumps. Two low-power 200-MeV beam dumps have been designed for the linac. Their function is to permit operation of

the linac for tune-up and improvements at the same time that workers are occupying the booster enclosure.

The nominal design beam power of the linac is 2.3 kW. The maximum beam power expected (in the same sense as in Sec. 4.1) is 30 kW. In order to avoid construction of a water-cooled dump, it was decided to limit the beam-power capacity of the dumps to 3 kW. We do not plan to operate the linac at high power levels without injecting the beam into the booster. Should it be necessary at a later time to test the linac at higher power levels, either of the two dumps can be easily removed and replaced by a water-cooled dump.

The size of the dumps designed for the linac is dictated by thermal considerations. Figure 8 is a cross-section view of the dumps. The main body is a solid cylindrical steel casting, which is embedded in a heavy-concrete block, as shown in the drawing.

An estimate has been made of the concentrations of radionuclides leaving the site in water via the aquifer at 690-ft elevation. The table below gives the ground-water data used in this estimate.

Ground-Water Data and Assumptions

Max. vertical ground-water velocity	8 ft/yr
Max. horizontal water velocity in aquifer	13 ft/day
Aquifer elevation	690 ft above msl
Beam-dump elevation	740 ft above msl
Neutron mean free path in soil, L	80 g/cm ²
Solubility fraction	0.1

The beam dump is taken to be a sphere of radius R in this model.

All the radionuclides are created in a disc of radius $R + 3L$ and height $2(R + 3L)$. While traversing this disc at 8 ft/yr, the activity reaches a maximum, then decays during the additional time needed to reach the site boundary. The dilution is calculated assuming the aquifer to be only 1 cm thick, which will give a large overestimation of the concentration. We find an activation time of 2.06 years, a decay time of 8.69 years, and a volume of water leaving the site of $5.45 \times 10^7 \text{ cm}^3/\text{yr}$. The table below lists the calculated concentrations of various radionuclides and compares them with the maximum permissible concentrations given in the AEC manual.

<u>Nuclide</u>	<u>Expected Concentration (p Ci/ml)</u>	<u>MPC (p Ci/ml)</u>	<u>Safety Factor</u>
^{55}Fe	5.9×10^{-3}	267	4.5×10^4
^{22}Na	1.5×10^{-3}	13	8.7×10^3
^3H	6.7×10^{-3}	1000	1.5×10^5
^{39}Ar	0.40×10^{-3}	--	
^{14}C	1.1×10^{-4}	267	2.4×10^6
^{41}Ca	0.38×10^{-4}	--	

There are apparently no problems of radionuclides arising from the linac beam dump.

b. Other Beam Dumps. The booster will have a beam dump similar in design to the linac dumps described above.

Work on main-accelerator, target, and experimental-area beam dumps is in progress at this time. An experiment has been carried out

in collaboration with personnel of the Argonne National Laboratory to measure leaching of radionuclides from the soil by ground water. This leaching and transport of radionuclides is an important problem for environmental protection of the general area of the site. An account of this work will be available in the near future.

4.4 Muon Shielding*

Muon shielding is a more important problem at NAL than at previous high-energy accelerators, because more muons are produced at higher energies and therefore have greater range. As seen in the discussion of main-accelerator shielding in Sec. 4.2, muons are not an important problem in the accelerator itself, because of their strongly forward production. For this same reason, they are an important problem in the areas of targets and experimental areas.

Muon shielding in these areas has not been designed in detail as yet, but considerable effort has been going into design studies of the physics problems of muon shielding. Most of these studies have been concerned with problems of homogeneous shields. Some studies have been made of active magnetized-iron shields, but they do not at this time appear economically justifiable.

Muon-transport programs¹⁸ have been made available to us by the Oak Ridge National Laboratory. A series of computations in

*This section is a summary of Ref. 17.

homogeneous soil shields has been carried out with the following assumptions:

(i) A cylindrical decay space in the target box, usually 600 cm long and 30 cm in diameter.

(ii) Pion production using the Trilling formula.¹⁹

(iii) dE/dx including correction for density effect in collision losses, bremsstrahlung, pair production, and nuclear interactions.

(iv) Multiple Coulomb scattering with energy loss after Eyges.²⁰

Some of the results for homogeneous shields are given in the next several figures. Figure 9 shows isoflux curves for the usual target geometry, while Fig. 10 shows the effects of varying the target geometry. The bulk of the shield is apparently insensitive to dramatic changes in target geometry.

Figure 11 shows the contributions from different production angles. Note that there is a large overlap caused by Coulomb scattering. The central small-angle ($\theta < 0.025$) contribution scatters far outside the 25-mrad line, while the large-angle ($\theta > 0.025$) contribution does not fall to zero at $\theta = 0$.

The effect of different target materials has also been investigated, as can be seen in Fig. 12, which compares the 10^{-13} isoflux line for Be and Pb. Larger shields are needed to absorb the higher-energy muons that are produced from a low-Z target according to the production model. At large depths in the shield, there are 1.6 ± 0.1 times more muons from the Be target than from the Pb target.

We do not expect that changes in the pion-production model will have major effects on the results. The disagreement between various models is mostly at the extreme high-energy end, where the total production is relatively small.

There are large fluctuations in the energy loss from bremsstrahlung, pair production, and nuclear interactions, and, consequently, there is large range straggling. In Fig. 13, we show results calculated using dE/dx from collisions alone, which should have less straggling, but a greater range. The shield length is therefore increased from 935 ft to 1000 ft. The radius of the shield also increases slightly at large depths in the shield.

To date, these calculations have been for ideal muon backstops -- without voids for beam pipes, beam-transport magnets, personnel-access entries, and so forth. These problems are under active study.

5. Beam-Loss Monitors

Because of the physical size of NAL and the large number of people at the Laboratory, it is important that there be an effective system for reporting beam losses to the accelerator operators and for stopping accelerator operation if the beam loss represents a hazard to people or equipment. But, again because of the great size of NAL, it is also important that the system be simple and inexpensive.

Development work has been carried out on such a beam-loss monitor. In this design, a 931A photomultiplier is mounted on the lid

of a quart container so that it hangs down into a high flash-point liquid scintillator which fills the container (an ordinary paint can). The photomultiplier could be dc-coupled to the multiplex data-transmission system that goes to the central-accelerator control room. Interlocks would be provided to shut down the ion source and/or accelerators if an abnormal, intolerable beam loss were detected.

Such detectors could be installed in the accelerator tunnels at appropriate intervals, perhaps every other magnet in the main accelerator. Prototypes of this monitor have been constructed and operated. The measured sensitivity is such that their signal-to-noise ratio is about 100 when beam loss is such that the remanent exposure rate is 2 mR/hr, one hour after shutdown at one foot from the magnets.

There will be places, such as beam-scrapers or extraction points, where this sensitivity is too large. We have also built and tested a low-sensitivity model, which is almost the same design except that no scintillator liquid is installed. These low-sensitivity devices will be installed where experience indicates larger beam losses are probable.

6. Personnel-Related Monitors

A system of colored film badges is being adopted to provide quick identification of workers' training and skills in radiation-exposure avoidance. Personnel dose records will be kept by the Radiation-Physics Section. Conventional film badges will be used until something better is developed.

A flexible gamma-insensitive portable neutron dosimeter (the Albatross) is being developed to give dose rate, occupancy time, integrated dose and integrated dose-alarms. This will be carried by accelerator-section personnel to work locations.

7. NAL Radiation-Safety Program

We repeat here an outline of Part 1 of the NAL Radiation-Safety Program, the document under which we are operating.

1.0 Policy

- 1.01 Protons shall not be accelerated unless there is a good use for them.
- 1.02 No person shall be exposed to radiation unnecessarily.
- 1.03 Radiation doses to individuals in controlled areas shall be limited to those maximum permissible doses set by the Federal Government.
- 1.04 The radiation levels in off-site areas and on-site areas open to the public, as well as general offices, shall not be greater than the limits set by the Federal Government for uncontrolled areas.
- 1.05 The beam dumps, accelerator, and external proton beam enclosures shall be so designed that normal radioactivation of the soil, known hydrology of the site, and foreseeable rainfalls will not contaminate above the permissible levels set by the Federal Government.
- 1.06 Proton beam losses shall be limited so that the remanent exposure rate inside the accelerator enclosures, including the external proton beam, shall safely permit all necessary maintenance.
- 1.07 Each person in the Laboratory is responsible for safety aspects of activities under his supervision.

8. Organization of Radiation-Safety Program

The ultimate responsibility for radiation safety at the National Accelerator Laboratory rests with the Laboratory Director. The Director shall delegate responsibility for the implementation of the Laboratory's radiation safety policies to the Radiation-Safety Officer, who shall report directly to the Director.

Under NAL's adopted system of organization, leaders of accelerator sections will be responsible for supervising the radiation safety of personnel in their sections. The Radiation-Physics Section will provide instrumentation, will train all Laboratory personnel who will be involved with radiation, and will supervise the implementation of the operational radiation-safety programs in each section.

We reproduce here sections from Parts 2 and 3 of the NAL Radiation-Safety Program. These define the responsibilities of the Radiation-Safety Officer and of the Section Heads and of the Laboratory's Radiation-Safety Committee.

- 2.2 The Radiation-Safety Officer will be charged with representing the Director for matters of radiation safety at NAL.
- 2.3 On behalf of the Director, the Radiation-Safety Officer or his delegate shall stop any activity which violates the Radiation-Safety Policy.
- 2.4 The Radiation-Safety Officer is responsible for the establishment and supervision of an operational radiation-safety program at NAL.
- 2.5 Included in the radiation-safety program are:

- 2.5.1 Organization and direction of a radiation-safety group of sufficient size to police radiation-producing activities of the Laboratory and to insure that equipment being used to monitor radiation is properly placed and calibrated.
 - 2.5.2 Maintenance of appropriate radiation records.
 - 2.5.3 Acquisition, distribution, and maintenance of suitable radiation-safety equipment.
 - 2.5.4 Acquisition and maintenance of radioactive sources for loaning to NAL personnel and visiting experimenters.
 - 2.5.5 Development of radiation-safety procedures in conjunction with the various section heads.
 - 2.5.6 Inspections and surveys to ascertain that established procedures and regulations are being observed.
 - 2.5.7 Supervision of the acquisition, handling, storing, and disposal of radioactive materials.
- 2.6 The Radiation-Safety Officer shall be readily available for consultation on radiation-safety matters. He shall be an ex-officio member of all groups planning or involved in activities where nuclear and/or x-ray radiations may be hazardous to the health.
- 2.7 The Radiation-Safety Officer shall maintain active programs for the development and refinement of radiation detectors, dosimeters, measurements of shielding characteristics, etc., and for the development of methods of calculating shielding, radioactivation doses, etc.
- 2.8 The Radiation-Safety Officer shall recommend to the Director the needed radiation-safety regulations for NAL.
- 2.9 With regard to Radiation Safety, each Section Head, in cooperation with and with the concurrence of the Radiation-Safety Officer, is responsible for:
- 2.9.1 Establishing and maintaining radiation safety in all areas in which members of his Section are active.

- 2.9.2 The installation and implementation of the radiation-safety program.
- 2.9.3 Development of operating procedures which include adequate provisions for radiation safety.
- 2.9.4 Supervision of the appropriate electrical, electronic, and other groups in the design, installation, maintenance, and periodic inspection of interlock and warning systems pertinent to radiation safety.
- 2.9.5 Supervision of operation of doors, gates, etc., leading to high-level radiation areas and of radiation-area warning signs as required.
- 2.9.6 Training of his Section's personnel in radiation-safety procedures, including engineers and technicians assigned to operating and controls crews.
- 2.9.7 Monitoring of radiation areas before personnel re-entries following operations and providing appropriate warnings and signals or dangerous levels of radioactivity.
- 2.9.8 Preparing detailed operating instructions for the radiation-safety equipment and the conduct of the safety program to guide the personnel.
- 2.9.9 Keeping records of radiation intensities in critical locations as instructed by the Radiation-Safety Officer.
- 2.9.10 Accomplishing either directly or with the assistance of the Radiation-Safety Officer, surveys of radioactive areas and devices, and establishing appropriate time-of-occupancy for maintenance personnel.
- 2.9.11 Keeping appropriate records of doses received by operating and maintenance personnel, which can be used as a guide in establishing personnel rotation.

2.9.12 Ascertaining that no materials, tools, accelerator components, instrumentation, or any other item that may have become radioactive above limits set by the Radiation-Safety Officer leaves the accelerator enclosures.

Activities equivalent to those in 2 to 12.

3.0 The Radiation-Safety Committee

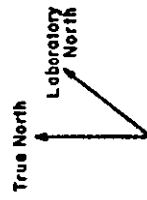
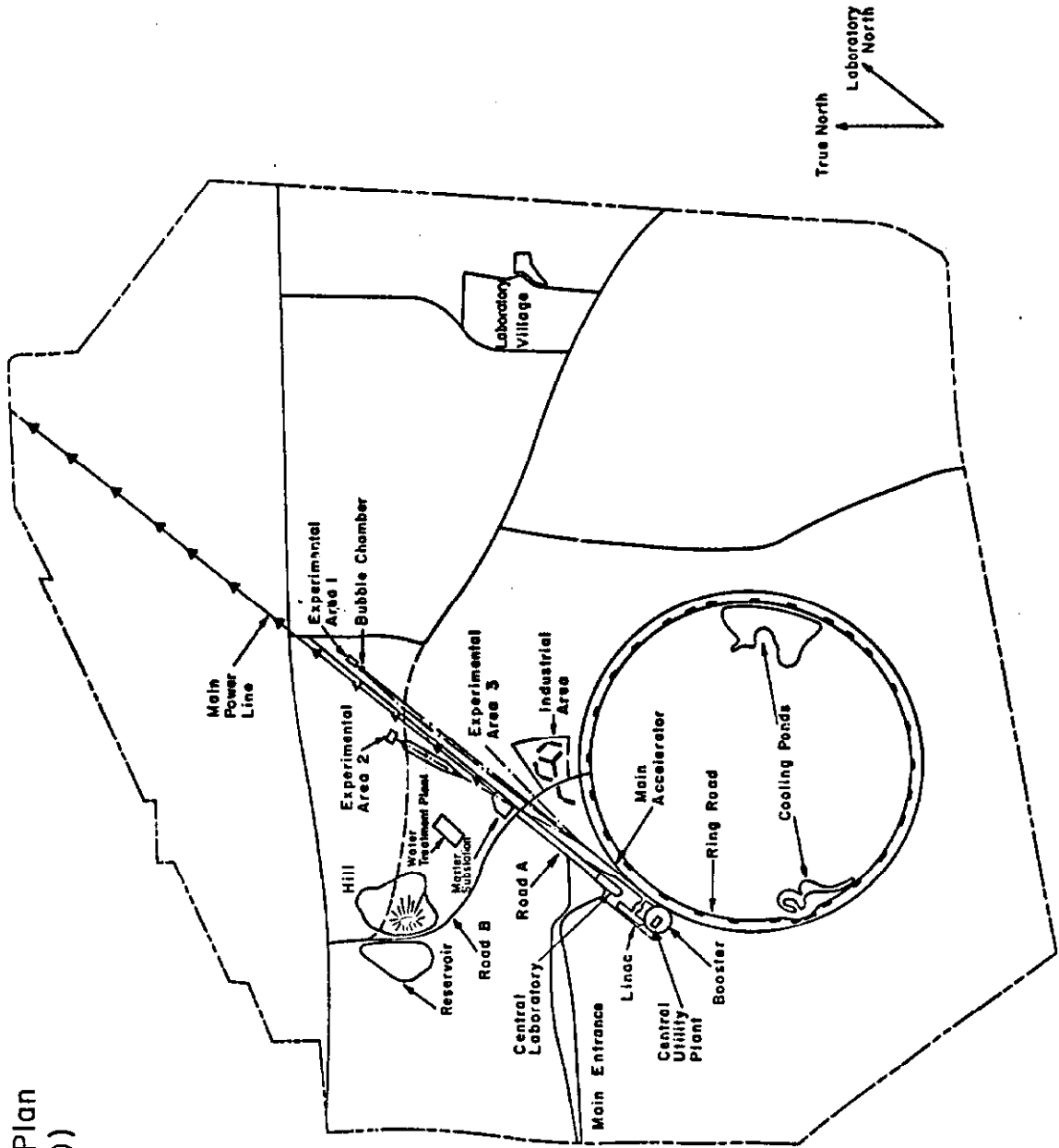
- 3.1 Purposes: The Radiation-Safety Committee shall meet as needed to deal with extraordinary matters. Meetings shall be called by the Chairman at the request of any of its members.
- 3.2 Membership: The Radiation-Safety Officer shall be the Chairman of the Radiation-Safety Committee. The Heads of the Accelerator Operations and Research Support Divisions as well as the Chairman of the Laboratory Safety Committee shall be ex-officio members of this Committee. Other members shall be appointed by the Director of NAL at his discretion.

REFERENCES

- ¹National Accelerator Laboratory Design Report, July, 1968.
- ²L. Blumberg to A. Maschke, private communication.
- ³M. Awschalom, Linac Shielding: Expected Beam Losses, Design Criteria, Tolerable Beam Losses, Radioactivation and Remanent Exposure Rate, Dose Rate to Beam-Loss Monitors, National Accelerator Laboratory Internal Report TM-236, May 5, 1970.
- ⁴K. O'Brien, Transverse Shielding Calculations for the Components of a 1/2 TeV Proton Synchrotron, HASL-199, August, 1968.
- ⁵R. G. Alsmiller et al., Analytical Representation of Nonelastic Cross Sections, Oak Ridge National Laboratory Report ORNL-4046, April, 1967.
- ⁶P. J. Gollon, Radioactivation of the NAL Linac by Proton Beam Losses: Design Criteria for a Beam Loss Monitoring System, National Accelerator Laboratory Internal Report TM-210, February 12, 1970.
- ⁷M. Awschalom, Lateral Shielding for the 8-GeV and 200-GeV Synchrotrons, National Accelerator Laboratory Internal Report TM-241, May 25, 1970.
- ⁸K. Goebel, private communication, April, 1968.
- ⁹T. W. Armstrong and R. G. Alsmiller, Calculation of the Residual Photon Dose Rate Around High-Energy Proton Accelerators, Oak Ridge National Laboratory Report ORNL-TM-2498, Feb. 10, 1969.

- ¹⁰T. W. Armstrong and J. Barish, Calculation of the Residual Photon Dose Rate Induced in Iron by 200-MeV Protons, Oak Ridge National Laboratory Report ORNL-TM-2583, May 2, 1969.
- ¹¹G. W. Wheeler, Shielding, Brookhaven National Laboratory Internal Memorandum, May 25, 1967.
- ¹²R. D. Fortune et al., Shielding Experiment at the CERN-PS, CERN/LRL/RHEL Collaboration, 1966; Lawrence Radiation Laboratory Report UCID-10199, April 28, 1967.
- ¹³G. Bellettini et al., Proton-Nuclei Cross Sections at 20 GeV, Nucl. Phys. 79, 609 (1966).
- ¹⁴P. J. Gollon and R. A. Carrigan, Jr., Design of Personnel and Vehicle Access Labyrinths, National Accelerator Laboratory Internal Report TM-239, May 5, 1970.
- ¹⁵F. Gervaise, M-M. d'Hombres, Variante du Programme ZEUS Appliquie à des Problemes de Tunnels: Programme ZEUS ALB. 5 et Programmes Auxiliares, Centre d'Etudes Nucleaires de Fontenay-aux-Roses Note CEA-N-933, 1968.
- ¹⁶R. E. Maerker, F. J. Muckenthalen, Calculation and Measurement of the Fast-Neutron Differential Dose Albedo for Concrete, Nucl. Sci. Eng. 22, 465 (1965).
- ¹⁷D. Theriot and M. Awschalom, Muon Shielding: Design Studies of Homogeneous Soil Shields at 200 GeV, National Accelerator Laboratory Internal Report TM-245, May 14, 1970.

- ¹⁸R. G. Alsmiller, Jr., M. Leimdorfer, and J. Barish, High Energy Muon Transport and the Muon Backstop for a 200-GeV Proton Accelerator, Oak Ridge National Laboratory Report ORNL-4322, Nov. 1968.
- ¹⁹J. Ranft and T. Borak, Improved Nucleon-Meson Cascade Calculations, National Accelerator Laboratory FN-193, Nov. 21, 1969.
- ²⁰L. Eyges, Phys. Rev. 74, 1534 (1948).



Master Site Plan
(April 1, 1970)



Fig. 1

FIGURE 2

NEUTRON DOSE RATE vs WALL THICKNESS
Solid Ordinary Concrete

$$dI/dl = 6.8 \times 10^8 \text{ protons cm}^{-1} \text{ sec}^{-1}$$

$$\text{Density of Concrete} = 2.3 \text{ gm cm}^{-1} \text{ sec}^{-1}$$

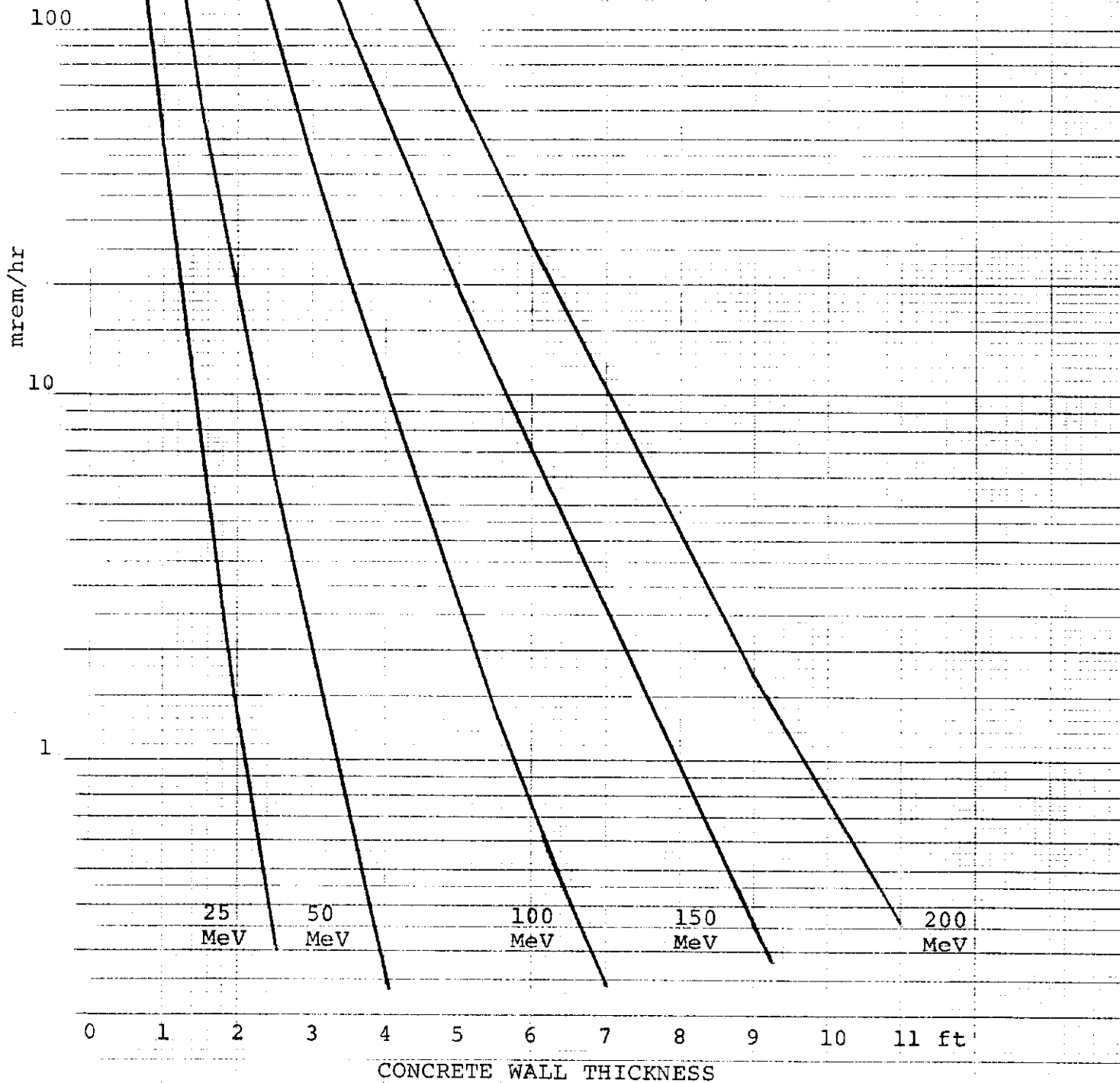


FIGURE 3

NEUTRON DOSE RATE vs WALL THICKNESS

3.0 ft Ordinary Concrete
+ Compacted Soil

$$dI/dl = 6.8 \times 10^8 \text{ protons cm}^{-1} \text{ sec}^{-1}$$

$$\text{Density of Concrete} = 2.3 \text{ gm cm}^{-3}$$

$$\text{Density of Soil} = 2.0 \text{ gm cm}^{-3}$$

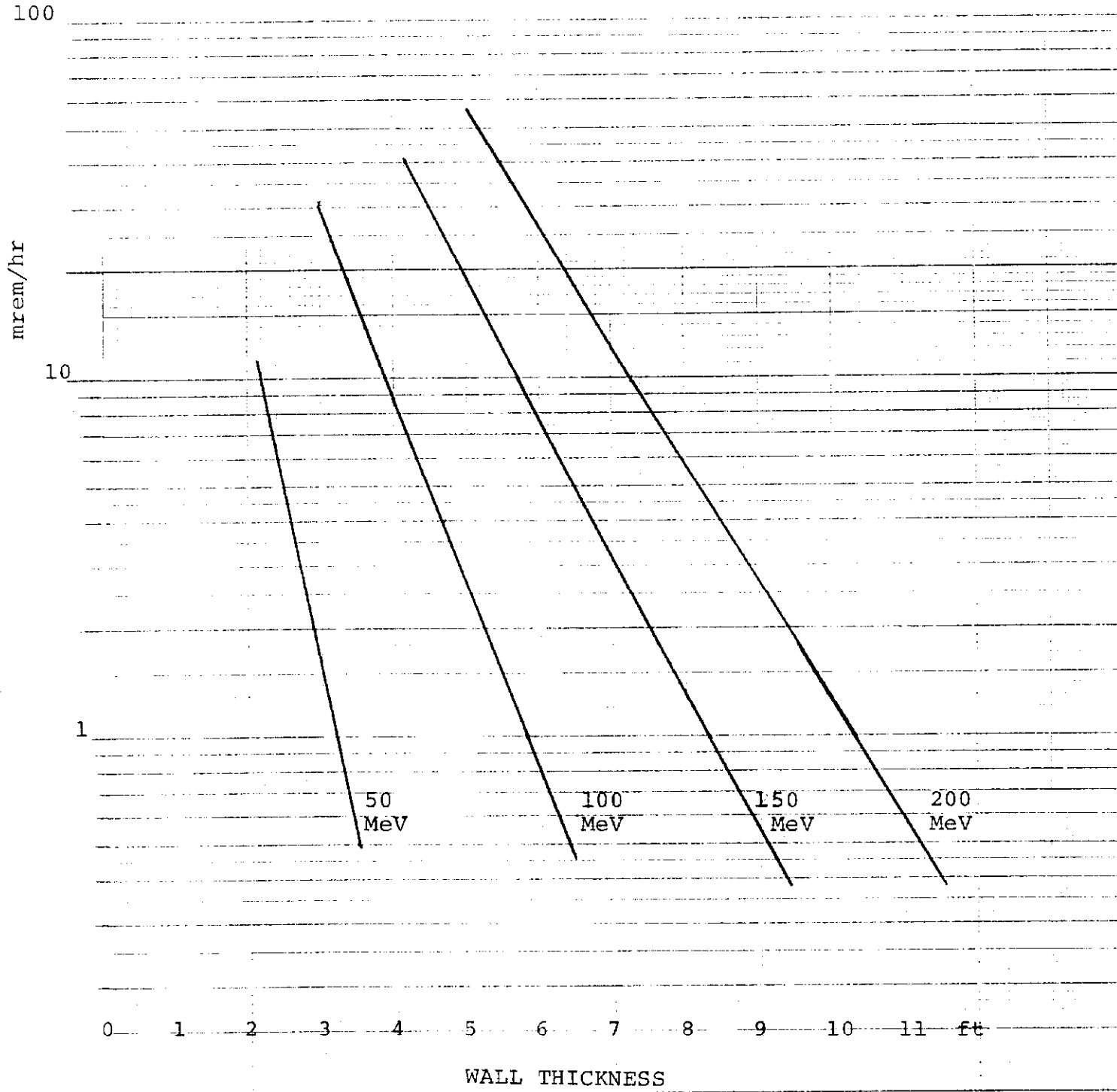


FIGURE 4

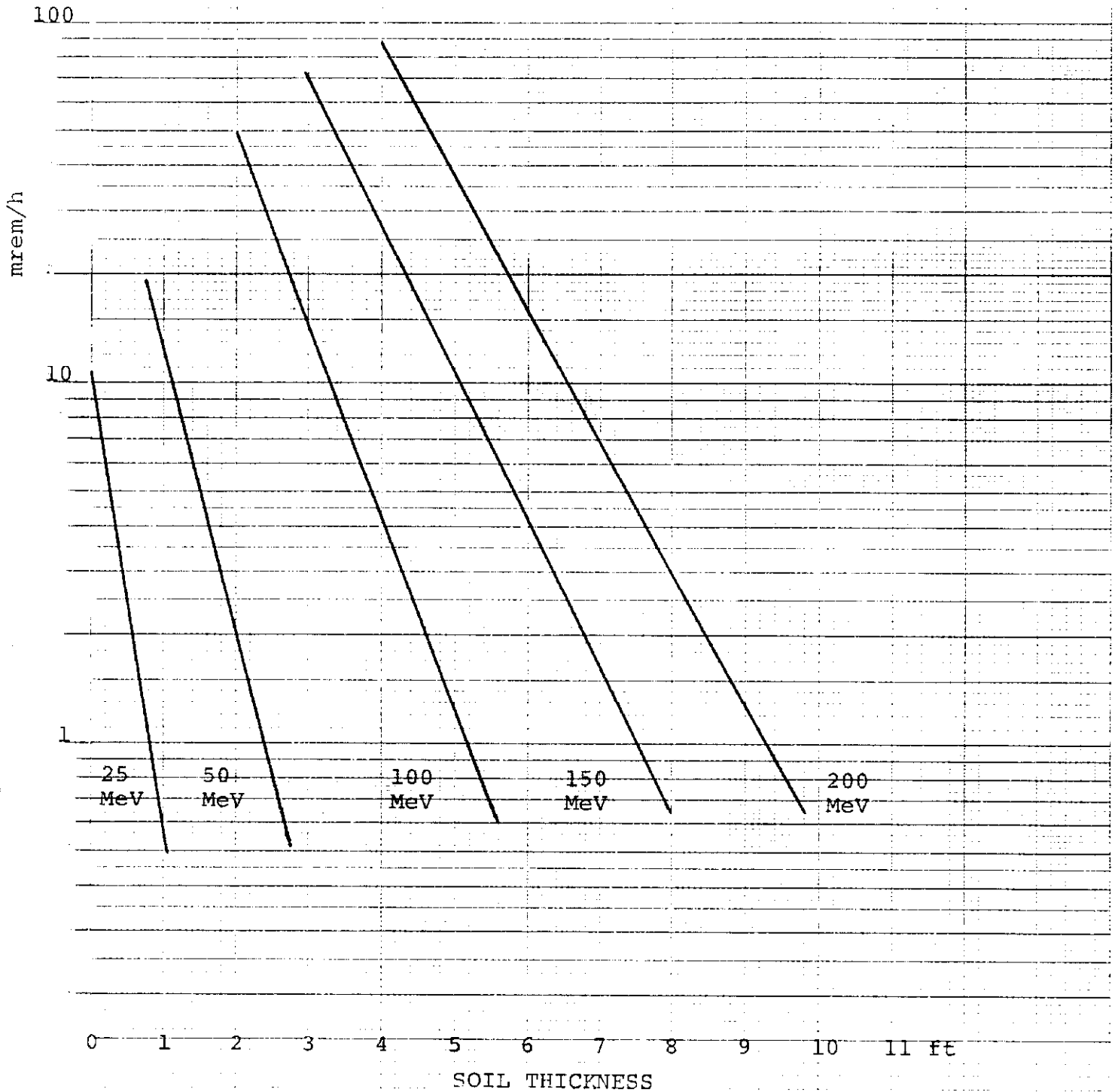
NEUTRON DOSE RATE vs BERM THICKNESS

1.5 ft Ordinary Concrete
+ Compacted Soil

$$dI/dl = 6.8 \times 10^8 \text{ protons cm}^{-1} \text{ sec}^{-1}$$

$$\text{Density of Concrete} = 2.3 \text{ gm cm}^{-3}$$

$$\text{Density of Soil} = 2.0 \text{ gm cm}^{-3}$$



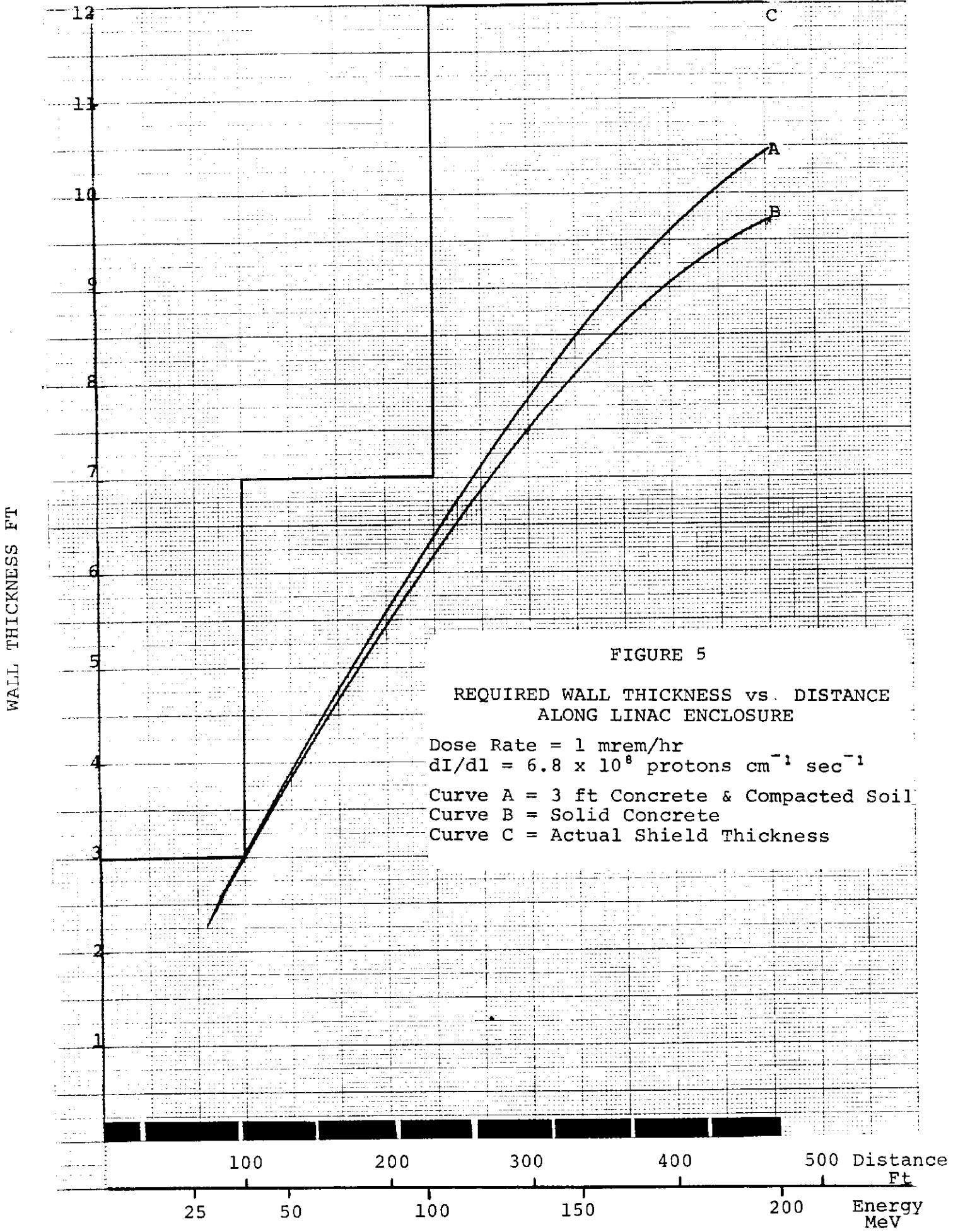


FIGURE 5

REQUIRED WALL THICKNESS vs. DISTANCE
ALONG LINAC ENCLOSURE

Dose Rate = 1 mrem/hr

$dI/dl = 6.8 \times 10^8 \text{ protons cm}^{-1} \text{ sec}^{-1}$

Curve A = 3 ft Concrete & Compacted Soil

Curve B = Solid Concrete

Curve C = Actual Shield Thickness

Figure 6. Major vehicle entrance to main accelerator enclosure. The stairs, elevator and hoist shaft leading down from the head house are not shown in the drawing, and were idealized into a single open shaft for purposes of calculation.

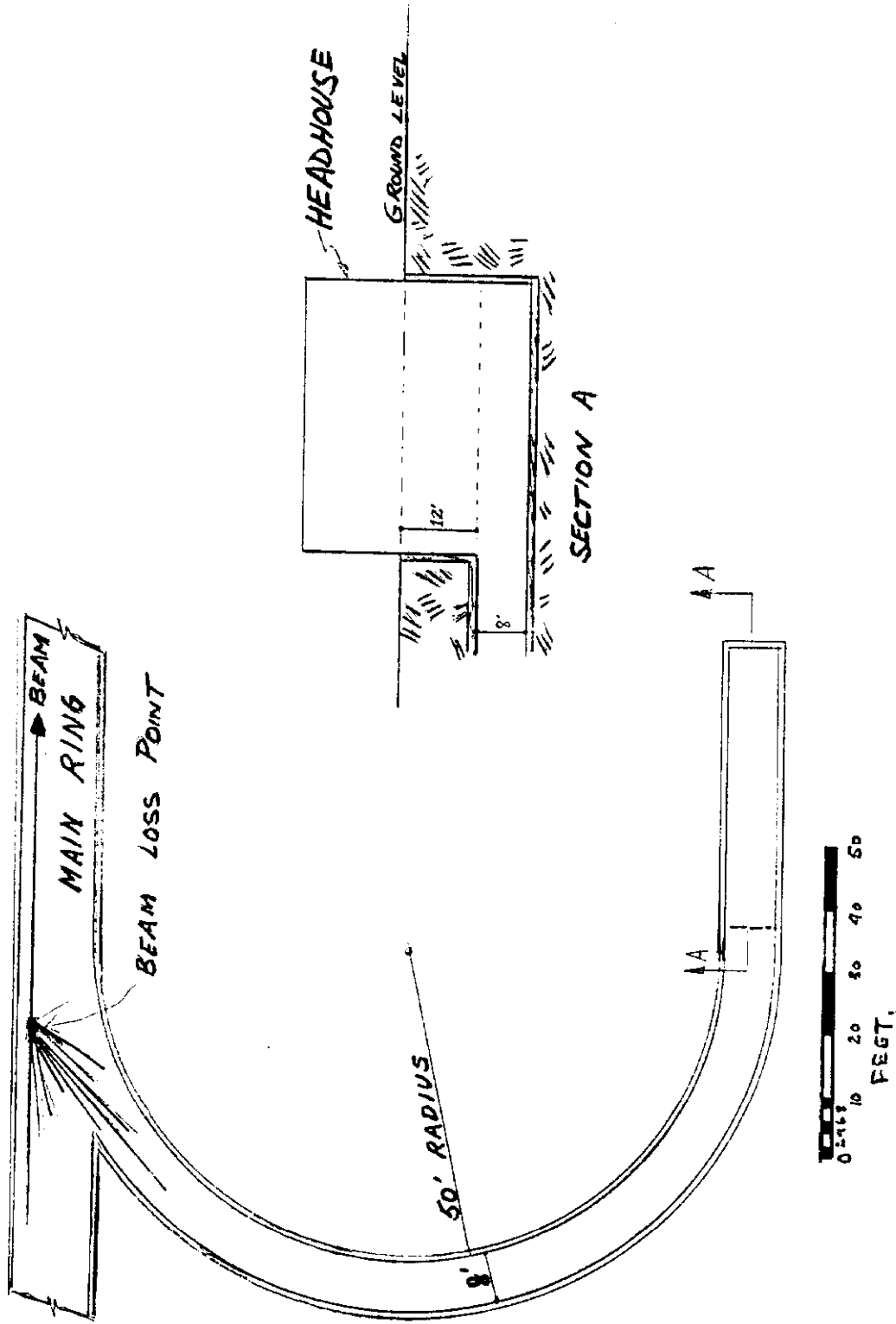
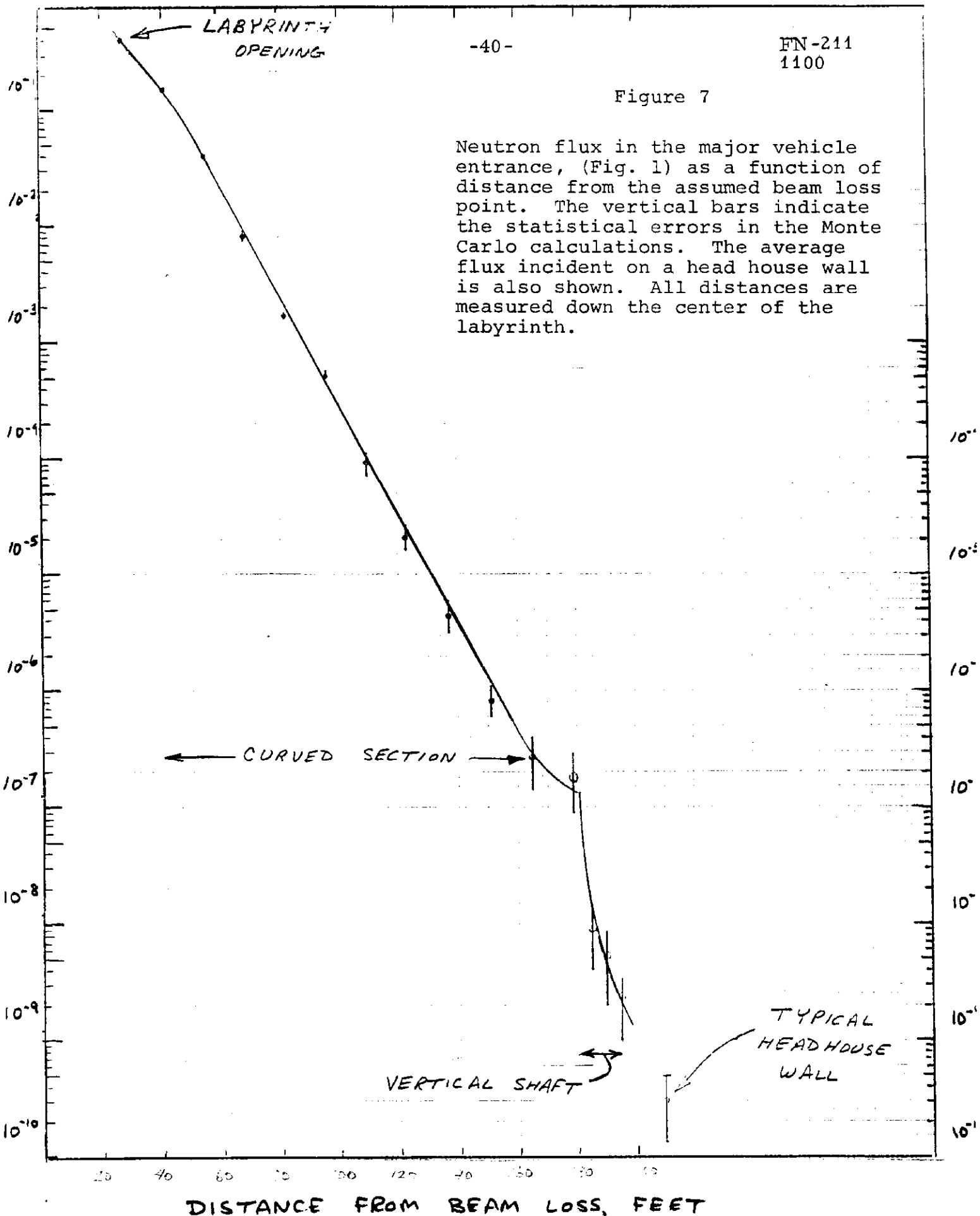


Figure 7

Neutron flux in the major vehicle entrance, (Fig. 1) as a function of distance from the assumed beam loss point. The vertical bars indicate the statistical errors in the Monte Carlo calculations. The average flux incident on a head house wall is also shown. All distances are measured down the center of the labyrinth.



DISTANCE FROM BEAM LOSS, FEET

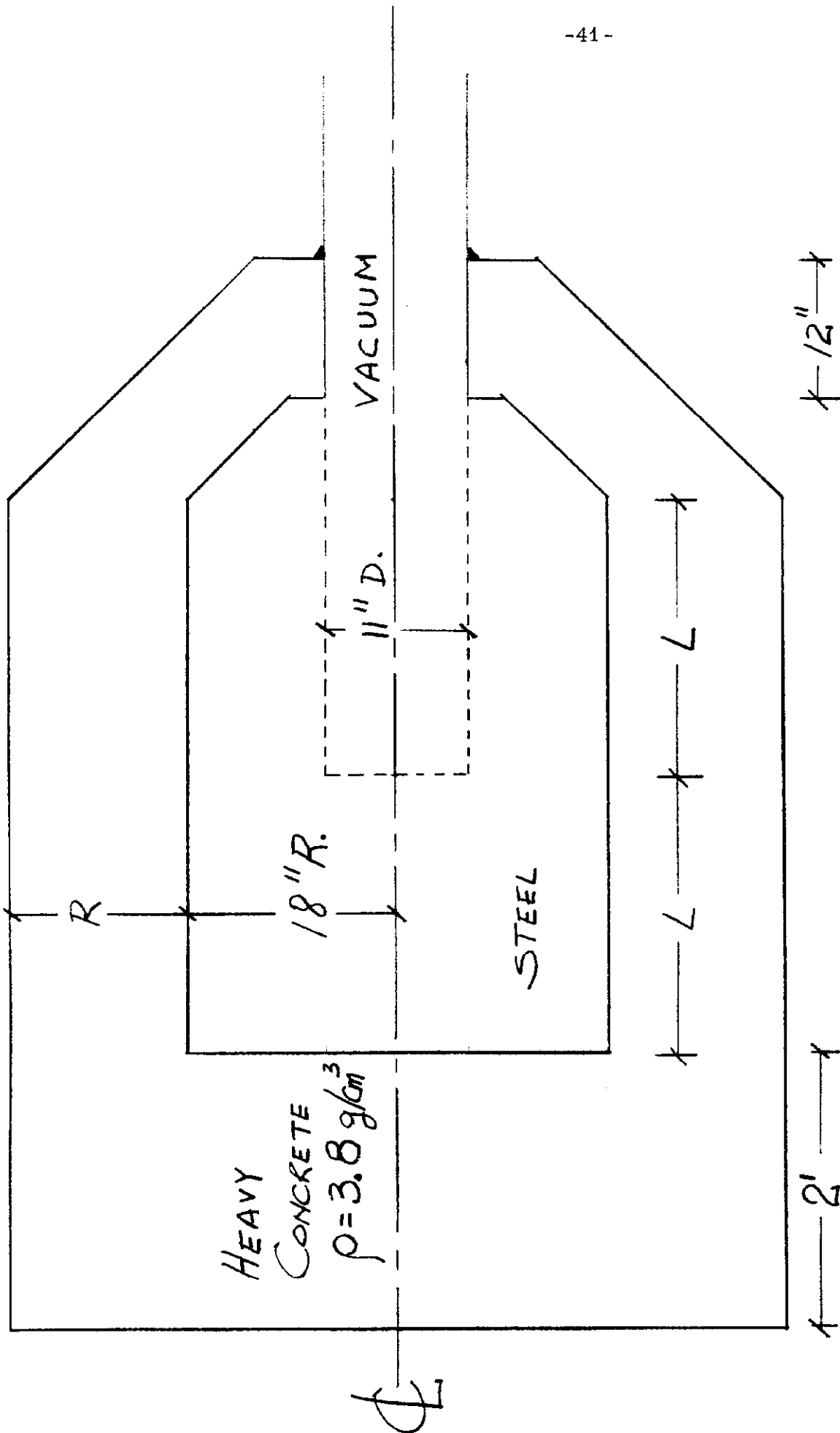
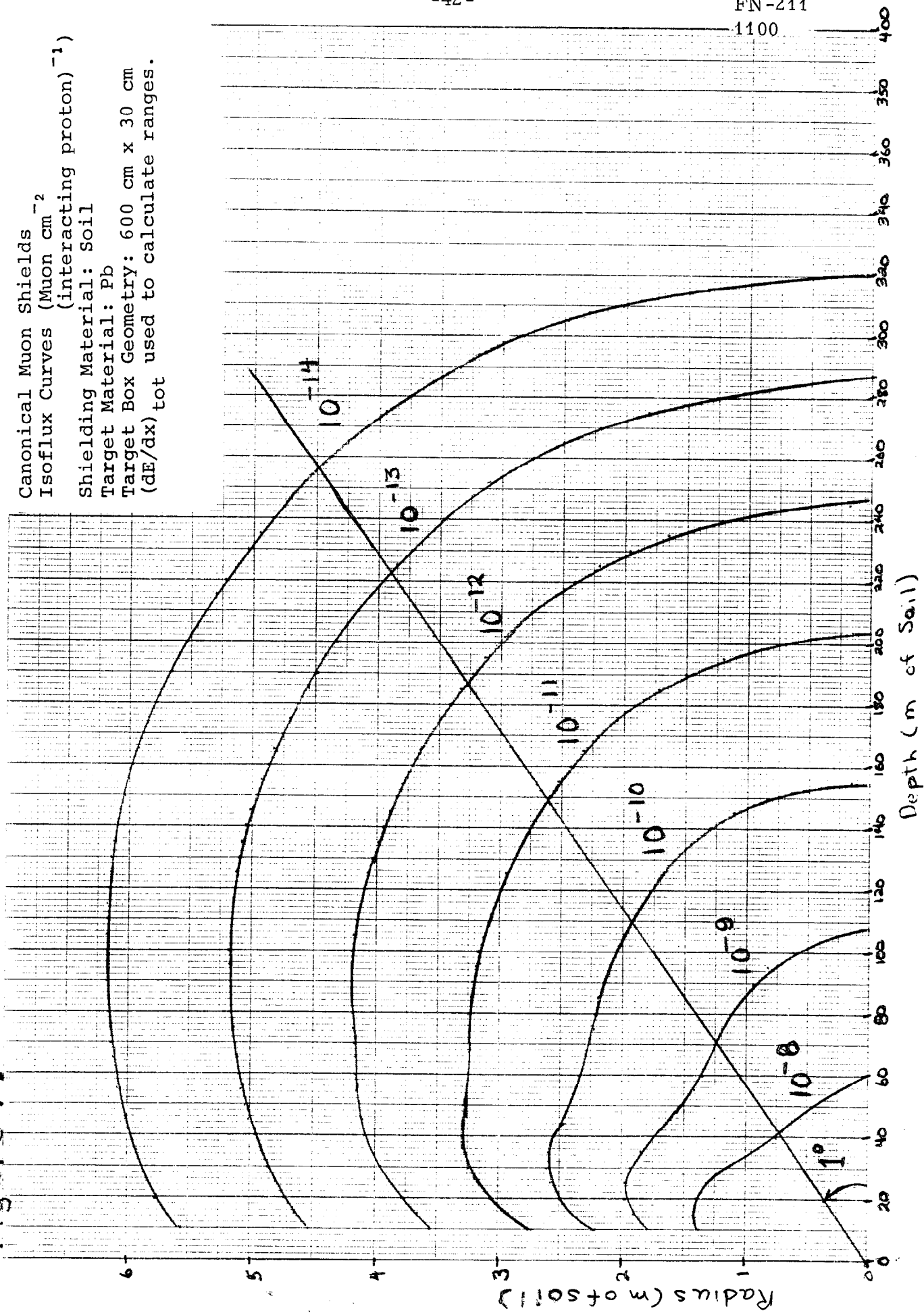


FIGURE 8. 200 MeV,
LINAC BEAM DUMPS.

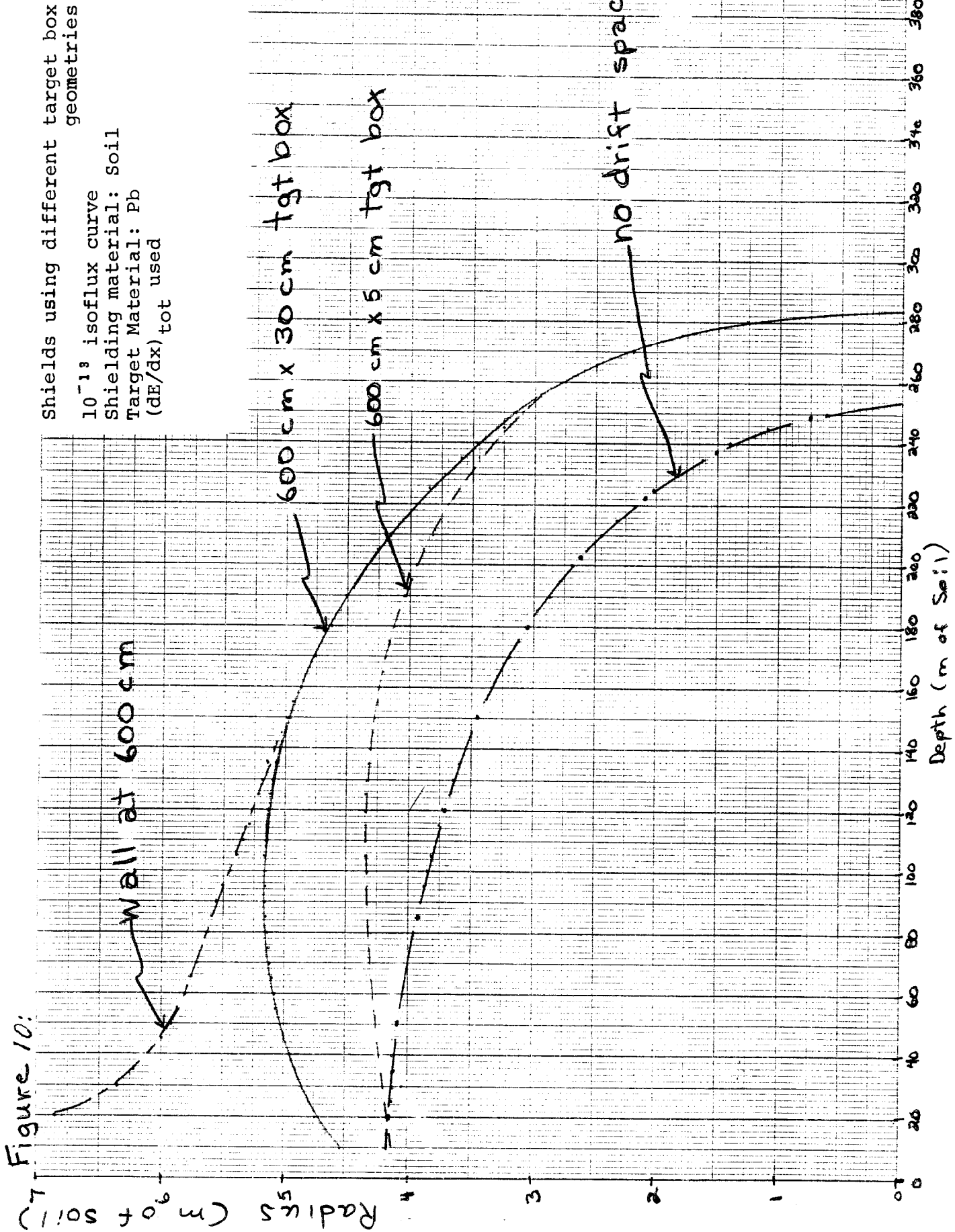
DUMP #1	L	3 ft	R	1 1/2 ft
DUMP #2	L	4 ft	R	1 1/4 ft

Figure 9:

Canonical Muon Shields cm^{-2}
 Isoflux Curves (Muon cm^{-2}
 (interacting proton) $^{-1}$)
 Shielding Material: Soil
 Target Material: Pb
 Target Box Geometry: 600 cm x 30 cm
 (dE/dx)_{tot} used to calculate ranges.

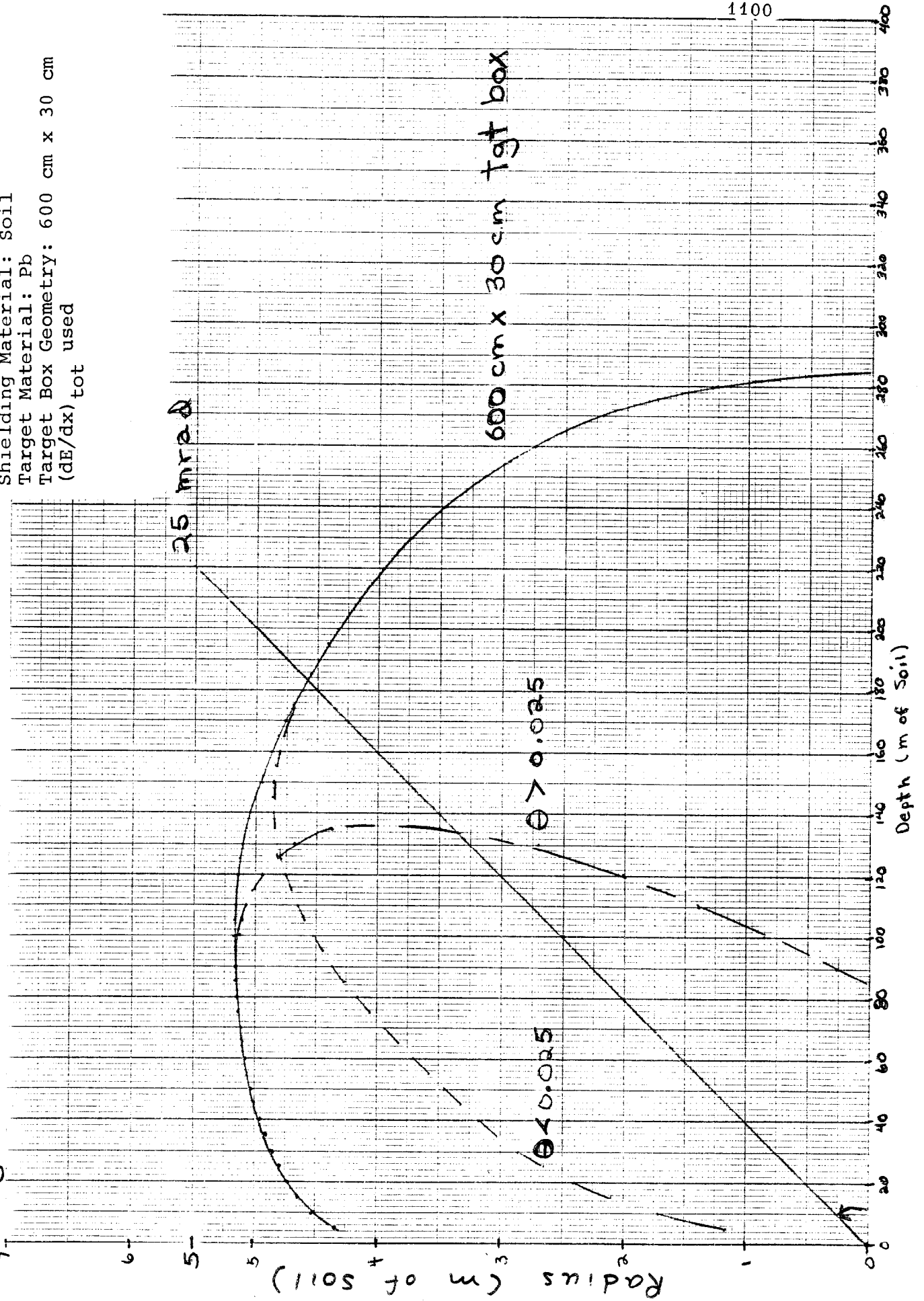


Depth (m of Soil)



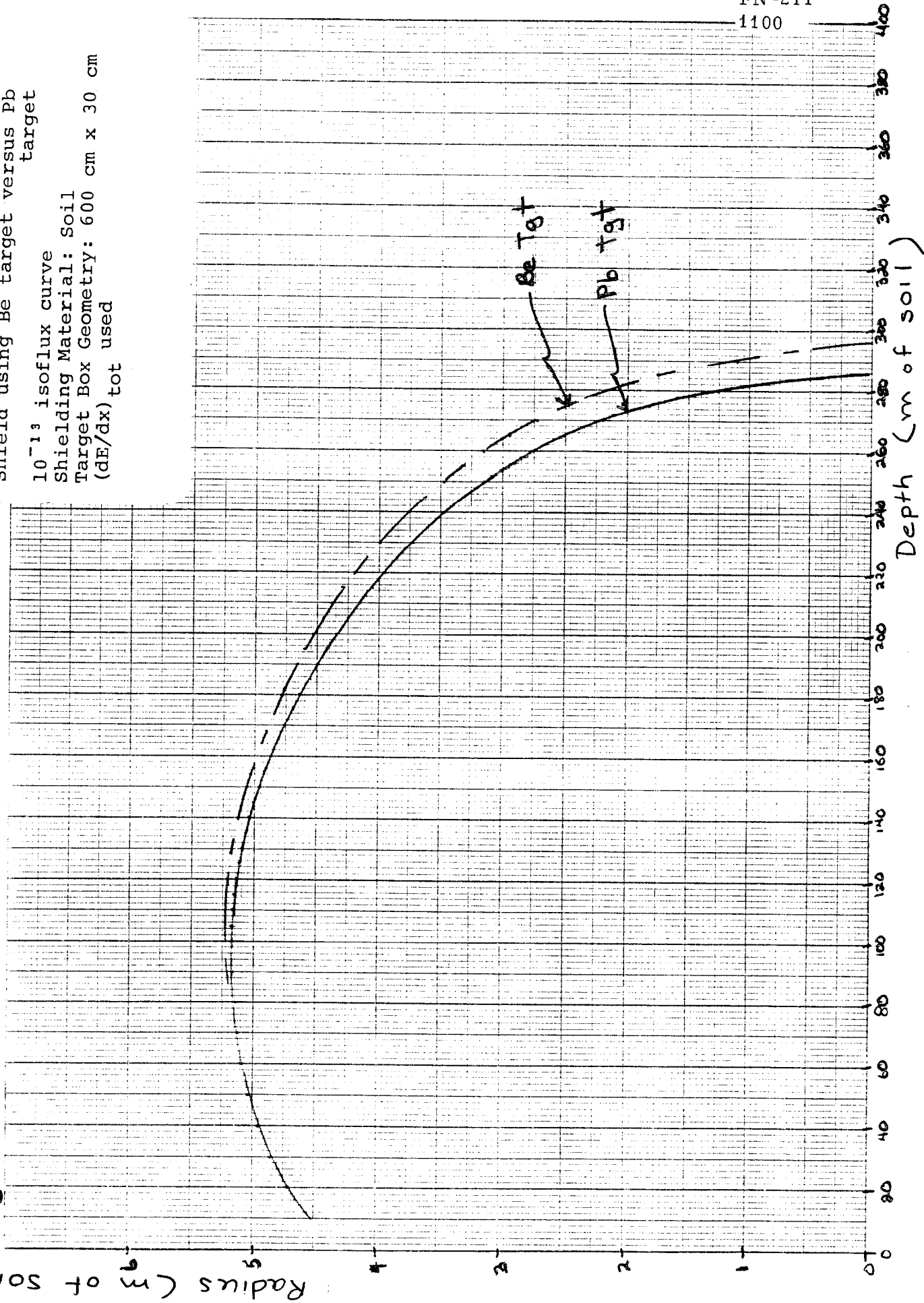
Two angular contributions to shield
10¹³ isoflux curve
Shielding Material: Soil
Target Material: Pb
Target Box Geometry: 600 cm x 30 cm
(dE/dx)_{tot} used

Figure 11:



Shield using Be target versus Pb target
 10^{-13} isoflux curve
Shielding Material: Soil
Target Box Geometry: 600 cm x 30 cm
(dE/dx)_{tot} used

Figure 12:



Shield using $(dE/dx)_{coll}$ versus
 $(dE/dx)_{tot}$
 10^{13} isoflux curve
 Shielding Material: Soil
 Target Material: Pb
 Target Box Geometry: 600 cm x 30 cm

Figure 13:

